

# A NOVEL METHOD TO COUPLE WELLBORE FLOW TO RESERVOIR FLOW

RAJESH J. PAWAR<sup>1</sup>,

GEORGE A. ZYVOLOSKI<sup>1</sup>

<sup>1</sup> *Hydrology, Geochemistry & Geology Group, Earth & Environment Sciences Division, Los Alamos National Laboratory, Los Alamos, NM – 87545, USA.*

## ABSTRACT

Incorporation of a wellbore to effectively capture near wellbore fluid flow physics has been one of the major challenges in porous media flow simulations. We have developed a computationally efficient method to couple wellbores to an existing numerical grid using FEHM (Finite Element Heat and Mass), the Los Alamos National Laboratory's numerical code for simulating heat and mass flow in porous media. The method effectively couples a radial solution for near wellbore flow with a control volume finite element solution for reservoir flow. Heat transfer and fluid flow in the vicinity of the wellbore are accurately represented with the method. It provides extreme flexibility to embed multiple wellbores at any desired locations in an existing numerical grid without a need for re-gridding. The method is capable of incorporating any desired wellbore fluid flow physics. Finally, the new method is computationally extremely efficient, requiring orders of magnitude less computational time compared to traditional methods for wellbore incorporation.

## 1. INTRODUCTION

It is important to capture the effects of changes in conditions near the wellbore in numerical reservoir simulations as they strongly affect the performance of the wellbore. One emerging area where accurately capturing the near wellbore reservoir behaviour may become important is geological sequestration of carbon dioxide (CO<sub>2</sub>). One of the major concerns of geologic sequestration is consequences of a failed wellbore and subsequent release of CO<sub>2</sub>. The release can be slow or catastrophic depending on the mode of wellbore failure. It is important to predict the release characteristics of a failed wellbore in order to develop monitoring plans, to understand potential impact and to develop strategies to mitigate the leak. For catastrophic leaks, the flow of CO<sub>2</sub> through the wellbore will strongly depend on the thermodynamic as well as the heat transfer and mass transfer processes near the wellbore, which makes effectively capturing the near wellbore conditions important.

Treatment of wells has been one of the major challenges in numerical simulations of fluid flow in porous media. Historically, wells have been incorporated through an equivalent radius expression to capture the physics of radial flow near wellbore (van Poolen et al., 1968; Peaceman, 1983). The equivalent radius was used to eliminate the need for solving a radial equation (for near wellbore domain) together with an equation for a reservoir grid. As these approaches average near wellbore conditions, they cannot effectively capture the true effects of large gradients in physical variables such as saturation and temperature. Alternate

approaches have been proposed to capture the changes near wellbore conditions, including coning models for multi-phase flow (Letkeman & Ridings, 1970; MacDonald & Coats, 1970; Settari & Aziz, 1974) as well as pseudo-functions. Local grid refinement methods such as those by Rosenberg (1982) and Heinemann et al. (1983) have been proposed to improve grid resolution near the wellbore. Pedrosa & Aziz (1986) and Hiebert et al. (1993) have proposed use of hybrid grids, which combine cylindrical and Cartesian grids to incorporate wellbores. The local grid refinement methods can result in a significantly large computational grid depending on the number of wellbores. In addition, both grid refinement and hybrid grid methods require either regriding or apriori knowledge of wellbore locations. For problems with multiple wellbores both regriding and hybrid grid methods could result in significant grid generation costs.

## 2. APPROACH

We have developed a new wellbore incorporation approach to overcome the limitations mentioned above. The approach is developed in FEHM (Finite Element Heat and Mass), a porous flow simulator developed at the Los Alamos National Laboratory. The wellbore incorporation algorithm was developed with following attributes:

- Ability to do a posteriori addition of wellbore to an existing grid at any desired location.
- Flexibility of computing the solution at any desired spatial resolution in the vicinity of the wellbore as well as in the wellbore.
- Ability to include wellbore complexities such as an annulus and physics such as turbulent flow.
- Ability to embed a radial wellbore patch in a much coarser 3-dimensional grid.
- Ability to perform computationally efficient and accurate simulation of short-term and long-term near wellbore processes.

The method depends strongly on the unstructured connectivity and control volume finite element (CVFE) approach of FEHM. The new algorithm is divided into 3 parts:

1. Define the wellbore and construct a grid.
2. Embed the wellbore grid in the primary grid.
3. Adjust resistance terms for primary grid.

### 2.1 Define the wellbore and construct the embedded grid.

The wellbore is defined as a wellbore patch, which consists of the wellbore itself and surrounding reservoir rock up to any desired radial extent. The user can define the details of the wellbore patch, including location of the wellbore, the radii of the wellbore and the outer patch, and the wellbore length (Figure 1a). In addition the user can also specify the total number of grid blocks in radial and vertical directions within the wellbore patch as well as the wellbore physics (i.e. laminar or turbulent flow). These details are defined in the input file after the primary grid is already defined.

### 2.2 Embed the wellbore grid in the primary grid.

The user-defined dimensions of the wellbore patch are used to generate a high-resolution 2-dimensional grid for the wellbore patch, which is embedded in the primary grid (Figure 1b & 1c). The process of connecting a high-resolution 2-dimensional radial grid into a 3-

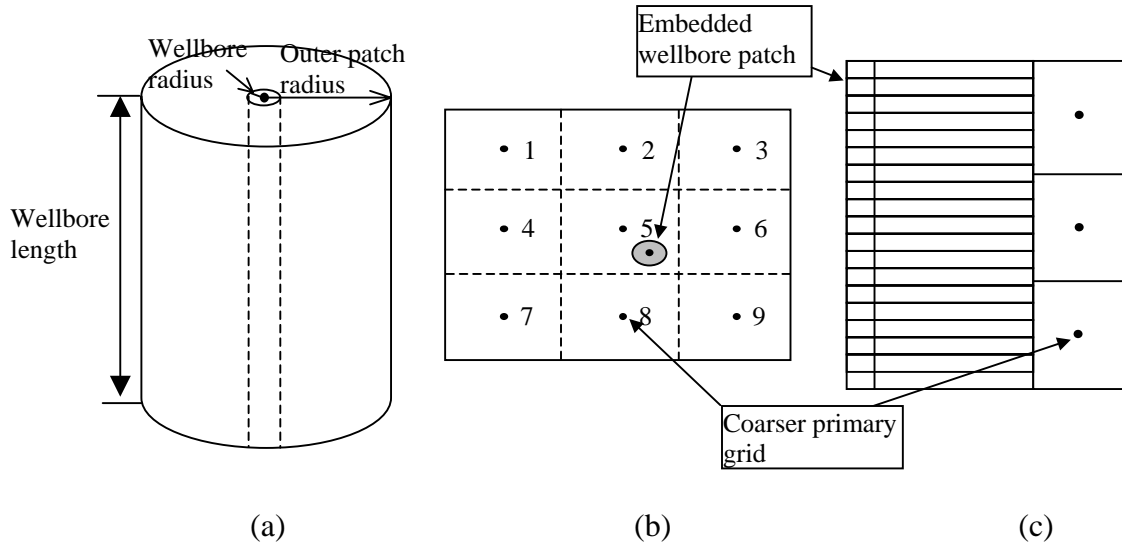


FIGURE 1. A schematic of the wellbore patch and the patch embedded in a coarser primary grid. Figure 1a shows details of the wellbore patch, 1b shows the embedded wellbore patch in a planar view, 1c shows the embedded wellbore patch in a vertical view.

dimensional primary grid poses no conceptual difficulties. The wellbore is embedded in a control volume, not a finite element. The wellbore and surrounding material does not need to be coincident with the primary grid block centre, both in planar and vertical directions. Because FEHM is a CVFE code, the volumes, areas and connectivity of the embedded grid are easy to generate. As the grid and associated volume for the wellbore patch are created, care is taken to insure that the corresponding volume is removed from the primary grid block in which the wellbore patch resides. At present, we allow the wellbore patch to traverse multiple control volumes in the vertical direction but constrain it to be contained in one grid block in the x-y plane. The outer most nodes of the wellbore patch are connected to the grid block in which the wellbore patch resides.

**2.3 Adjust inter-block transfer terms for primary grid.**

Before addressing the details of adjusting the inter-block transfer terms in the primary grid, it is instructive to first describe the control volume finite element (CVFE) technique. While finite difference (FD) and finite element (FE) methods are well understood, descriptions of CVFE techniques are not widely available. The origin of the method can be traced to early finite element applications to non-linear fluid flow problems (Dalen, 1979, and Zyvoloski, 1983). The method is described in some detail in Forsyth (1989). In simplistic terms, the CVFE method can be described as a block-centered finite difference method on irregularly shaped control volumes. Non-orthogonal connections are allowed so long as they have positive areas. The rules for node spacing and geometry were developed by Voronoi, (Voronoi, 1908). The Voronoi volume is formed by boundaries that are orthogonal to the lines joining adjacent nodes and that intersect the midpoints of the lines. The material balance equations that describe the flow of a fluid are discretized via CVFE method as;

$$V_i \frac{[(\rho\phi)^{n+1} - (\rho\phi)^n]}{\Delta t} = \sum_{j \in \eta_i} \left( \frac{k\rho}{\mu} \right)_{ij} \cdot \left( \frac{A_{ij}}{\Delta d_{ij}} \right) \cdot [(P_j - P_i) - (\rho g)_{ij} (z_j - z_i)] + q_i, \quad (1)$$

where,  $\eta_i$  is the set of neighbour nodes of  $i$ ,  $V_i$  is the Voronoi volume associated with node  $i$ ,  $A_{ij}$  is the area between connected nodes  $i$  and  $j$ ,  $d_{ij}$  is the distance between nodes  $i$  and  $j$ ,  $k$  is the permeability,  $\rho$  is the fluid density, and  $\mu$  is the fluid viscosity. Superscripts  $n$  and  $n+1$  indicate the successive time steps and  $q_i$  is the flow source or sink term. Important aspects of CVFE methods are that they support harmonic weighting of permeabilities and upwinding of nonlinear fluid properties. It is also important to note that when CVFE methods are applied to orthogonal finite difference grids they *exactly* reproduce the finite difference equations.

When embedding a wellbore patch, we modify the connectivities for the primary grid as follows (for simplicity we consider only x-y connections). Consider the center grid block (labeled '5') in Figure 1b. The difference formula in Eq. 1 may be written as:

$$\sum_{j=2,4,6,8} C_{ij} (P_j - P_5) \quad (2)$$

$$\text{where, } C_{i,j} = \left( \frac{k\rho}{\mu} \right)_{ij} \frac{A_{ij}}{d_{ij}}$$

First, we add additional connections to Eq. 2 of the form:

$$C_{i,w} (P_w - P_5) \quad (3)$$

where,  $P_w$  is the pressure of an outside node of the embedded grid. Note that several embedded grid nodes can be attached to the same primary grid node. Figure 1c shows a very abrupt change in resolution between the primary and embedded grid. We assume that the radial grid extends far enough from the wellbore that the loss of accuracy in the averaging between the coarse and fine grids is less than other errors. The  $C_{i,w}$  term in Eq.3 is large compared with the other  $C_{i,j}$  terms associated with node 5. This ensures that the pressure drop or temperature change is minimal between the wellbore and the grid block centre. Algebraically, this is equivalent to moving the wellbore grid to the primary grid block centre. The fact that the wellbore system is not centred is accounted for by influence factors, which are applied to modify the primary grid block connections. Next, we modify the  $C_{i,j}$  terms for the primary grid blocks. When the wellbore is coincident with the block centre, we modify the area and distance between adjacent primary grid blocks in a symmetric manner. When the wellbore patch is not centred in the primary grid block we the influence factors mentioned above are employed to preferentially weigh primary grid blocks.

### 3. RESULTS

In order to insure that the radial portion of our formulation (representing the wellbore patch) was being calculated correctly, we compared the solution for the embedded grid with a solution for a radial grid. The radial grid had same dimensions as the wellbore patch and no

connections such as those between the outside nodes of the wellbore patch and primary grid nodes for the embedded grid. The problem definition was as follows. A wellbore was embedded in a primary Cartesian grid. The primary grid had 11 x 11 x 11 nodes in x, y and z directions, respectively. The primary grid block dimensions were 495 meters x 495 meters x 10 meters. A wellbore of 10 cm internal diameter was placed at the node in the centre of the primary grid. A volume with outer radius of 206.25 meters from the wellbore centre was identified as the wellbore patch. To better capture the behaviour closer to the wellbore, the wellbore patch was further refined in 10 radial elements. Similar to the primary grid, the wellbore also had 11 nodes in the 'z' direction placed exactly at the same location as the primary grid nodes. Note that the above-mentioned wellbore patch was specified through the input file and not by regriding the primary grid. The porosity for the wellbore nodes was 100%. The vertical and horizontal permeability for the wellbore nodes was  $10^{-10}$  and  $10^{-18}$  m<sup>2</sup>, respectively. The reservoir was initially at 1 MPa and 100 °C. Water at 20 °C was injected through the top well bore node at a rate of 0.2 kg/s and change in the reservoir temperature over time was calculated for two different types of problems. First, we compared the solutions for the case where the injected water flowed through the wellbore and out of the wellbore from the bottom wellbore node (Figure 2a). This was done by holding the pressure at the bottom well bore node constant at 1 MPa. There was only heat transfer between wellbore nodes and surrounding reservoir nodes. The mass transfer was limited by keeping the reservoir porosity at 0%. In the second problem, the horizontal permeability in the bottom wellbore node was increased from  $10^{-18}$  m<sup>2</sup> to  $10^{-14}$  m<sup>2</sup> and the reservoir porosity was increased to 20%. For this problem the boundary condition was changed such that the water flowed down the wellbore and in the reservoir from the bottom wellbore node (Figure 2b).

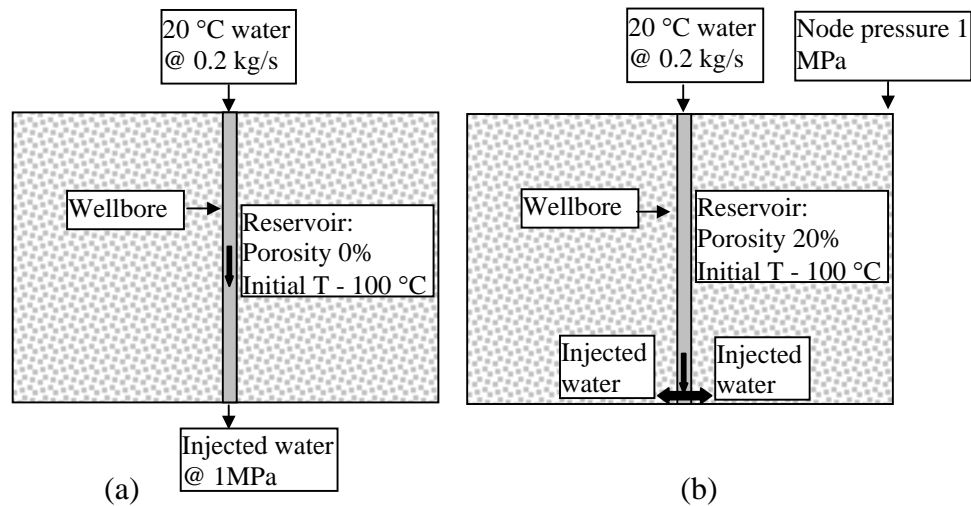


FIGURE 2. A schematic diagram showing the configuration of the comparison problems. Figure 2a shows configuration for heat transfer only problem where water flows only through the wellbore. Figure 2b shows the configuration for heat and mass transfer problem where water flows through the wellbore and in the reservoir through the bottom node.

Comparison of the temperature profiles near the wellbore region after 10,000 days of cold-water injection are shown in Figures 3a and 3b. Figure 3a shows the comparison for heat

transfer only problem described in Figure 2a, while Figure 3b shows the comparison for heat and mass transfer problem described in Figure 2b.

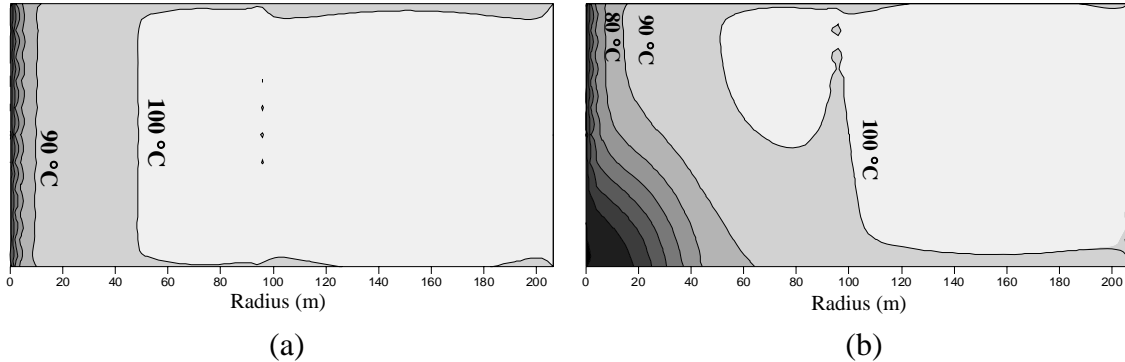


FIGURE 3. Comparison of temperature profiles along the radial direction. The wellbore is at 0 m. The solid lines show the contours for embedded wellbore patch. The filled contours show the contours for radial grid used for comparison. Figure 3a shows results for heat transfer only problem. Figure 3b shows results for heat and mass transfer problem.

As can be seen from the two figures, the radial solution is very well re-produced for the wellbore patch in the new formulation.

After confirming that the radial flow is accurately captured, we compared the computational performance of the new formulation against other approaches for incorporating the wellbore. For this comparison we used a different problem formulation. A wellbore patch was embedded in a 26x26x11 primary grid. The primary grid block dimensions were 200 meters in x and y directions and 10 meters in the z direction. A wellbore patch was embedded in the primary grid at the grid block located at (2400, 2400). The wellbore patch consisted of a wellbore of 0.226 meter radius. In addition, the patch included the reservoir region within the 100 meters radius from the wellbore centre. The wellbore patch was further divided along 10 nodes in radial direction. Similar to the earlier problem, the wellbore patch was defined through the input file and not by regriding the primary grid. We compared solution for this grid with three other configurations for wellbore representation as follows:

1. A hybrid grid formulation, which represented the wellbore and area around it by a cylindrical grid and the reservoir by a cartesian grid. The cylindrical grid was at the same resolution as the wellbore patch in the grid for new formulation. The inside cylinder representing the wellbore had radius of 0.226 meter.
2. A refined finite difference grid, which had 200 meters primary grid spacing. The block at (2400, 2400) was further refined in 16 grid blocks in x and y directions. The refinement was done such that the inner most grid block which represented the well bore was 0.4 meter in x and y directions. This resulted in same well bore cross-sectional area and volume as the other formulations.
3. An octree refined grid, which used a locally refined octree grid at the grid block at (2400, 2400). Similar to the finite difference grid, the refinement was done such that the grid block representing the well bore was 0.4 meter in x and y directions.

We compared the solution for the combined heat and mass transfer problem (Figure 2b) with these different wellbore incorporation methods. Evolution of temperature profiles was

studied where water at 20 °C was injected for 10000 days in a formation initially at 100 °C. The water flowed through the wellbore and in the reservoir through the bottom wellbore node. The results are shown in Figure 4.

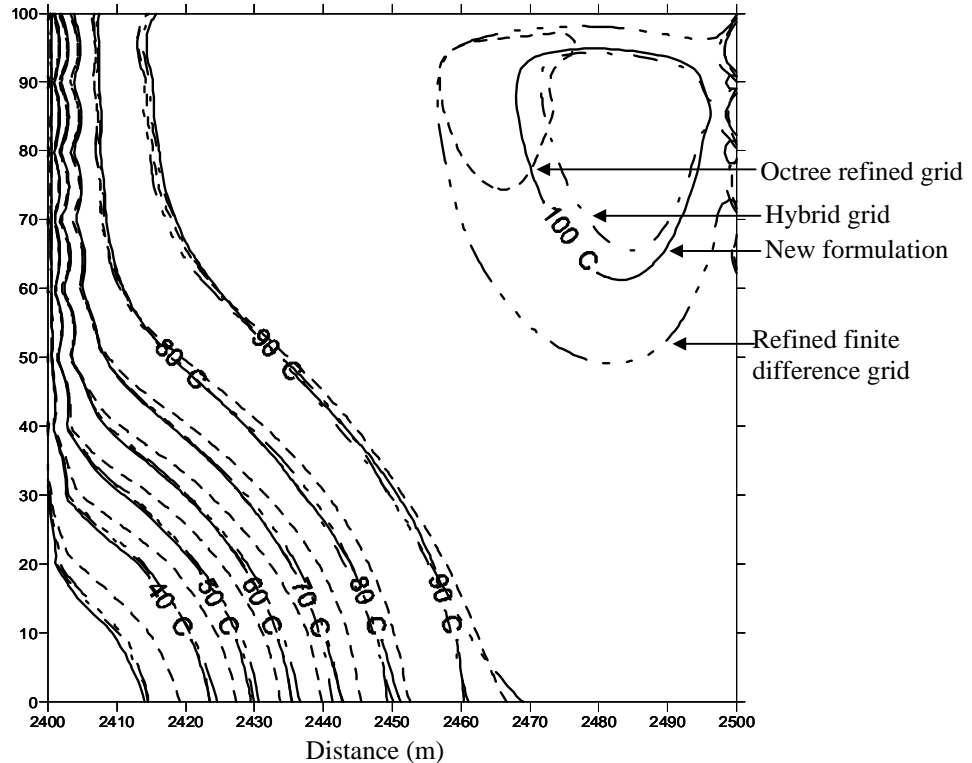


FIGURE 4. Comparison of temperature profiles near the wellbore (at 2400 m) along a vertical plane. Solid lines show contours for new formulation, dash-dot lines show contours for hybrid grid, uniform dashed lines show contours for octree refined grid and mixed dashed lines show contours for refined finite difference grid.

Overall, the solution from the new formulation matches the other solutions very well. The match is much better with solution for the hybrid grid than the other two formulations. This could be because both the new formulation and hybrid grid formulation have radial flow physics near the wellbore, while the other two don't. Table 1 compares the numerics for the four formulations. As can be seen from the table, the new formulation is computationally extremely efficient compared to the grid refinement formulations. The computational performance of the hybrid grid formulation is comparable to the new formulation. On the other hand, incorporation of wellbore with hybrid grid formulation required regridding the entire grid. Depending on the number of wellbores this can result in significant gridding effort.

TABLE 1. Comparison of numerics for the four different formulations for wellbore incorporation.

Problem Formulation	Total number of grid blocks	Computational Time (sec)	Total number of Newton-Raphson iterations
New formulation	7436	37	102
Hybrid grid	8316	46	101
Refined FD grid	19404	403	181
Octree refined grid	12980	1645	430

#### 4. CONCLUSIONS

We have developed a novel method to incorporate wellbores in reservoir simulation problem. The new method provides extreme flexibility when defining a wellbore. Incorporation of wellbores does not require any regridding of the primary grid. The formulation provides capability to study near wellbore processes at any desired spatial resolution. The new formulation in effect combines a radial solution with a control volume finite element solution to capture the radial nature of fluid flow near wellbores. Comparison of the solutions with the new formulation to the solution with a radial grid formulation confirms that the new formulation can accurately capture near wellbore radial behaviour. The new formulation is also computationally extremely efficient and is orders of magnitude faster compared to some of the traditional methods of wellbore incorporation.

#### REFERENCES

- Dalen, V. (1979), Simplified finite element models for reservoir flow problems, *SPEJ*, 19 (5), 333-343.
- Forsyth, P. A. (1989), Control volume finite element method for local mesh refinement, paper presented at the Symposium on Reservoir Simulation, Society of Petroleum Engineers, Houston, Tex., 6-8, February.
- Heinemann, Z. E., G. Gerken and G. von Hantelmann (1983), Using local grid refinement in a multiple application reservoir simulator, paper presented at the Symposium on Reservoir Simulation, Society of Petroleum Engineers, San Francisco, Calif., 15-18, November.
- Hiebert, A. D., L. S. K. Fung, V. Oballa, and F. M. Mourits (1993), Comparison of discretization methods for modelling near-well phenomena in thermal processes, *J. Can. Pet. Tech.*, 32 (3), 46-52.
- Letkeman, J. P. and R. L. Ridings (1970), A numerical coning model, *SPEJ*, 10 (4), 418-424.
- MacDonald, R. C. and K. H. Coats (1970), Methods for numerical simulation of water and gas coning, *SPEJ*, 10 (4), 425-436.
- Peaceman, D. W. (1983), Interpretation of wellblock pressures in numerical reservoir simulation with nonsquare gridblocks and anisotropic permeability, *SPEJ*, 23 (3), 531-543.
- Pedrosa, O. A. Jr. and K. Aziz (1986), Use of a hybrid grid in reservoir simulation, *SPERE*, 1 (6), 611-621.
- Rosenberg, D. U. (1982), Local mesh refinement for finite difference methods, paper presented at the Annual Technical Conference and Exhibition, Society of Petroleum Engineers, New Orleans, Louis., 26-29, September.
- Settari, A. and K. Aziz (1974), A computer model for two phase coning simulation, *SPEJ*, 14 (3), 221-236.
- van Poollen, H. K., E. A. Breitenback, and D. H. Thurnau (1968), Treatment of individual wells and grids in reservoir modelling, *SPEJ*, 8 (4), 341-346.
- Voronoi, G. (1908), Nouvelles applications des paramtres continues a la theorie des formes quadratiques, *J. Reine Angew Mathe*, 134, 198-287.
- Zyvoloski, G. (1983), Finite element methods for geothermal reservoir simulation, *Int. J. Numer Anal Methods Geomech*, 7 (1), 75-86.